Chapter 19
Implementation of Simplified Models of Local Controller for Multi-terminal HVDC Systems in DIgSILENT PowerFactory

Francisco M. Gonzalez-Longatt, J.M. Roldan, José Luis Rueda, C.A. Charalambous and B.S. Rajpurohit

Abstract The North Sea has a vast potential for renewable energy generation: offshore wind power, tidal and wave energy. The voltage source converter (VSC) and high voltage direct current (HVDC) systems are more flexible than their AC counterparts. This offers distinct advantages for integrating offshore wind farms to inland grid system. It seems that advances on technologies open the door for VSC-HVDC systems at higher voltage and at higher power range, which is making multi-terminal HVDC (MTDC) system technically feasible. The control system for MTDC consists of a central master controller and local terminal controllers at the site of each converter station. The terminal controllers (outer controllers) are mainly responsible

F.M. Gonzalez-Longatt (✉)
School of Electronic, Electrical and Systems Engineering, Loughborough University, LE11 3TU Loughborough, UK
e-mail: fglongatt@fglongatt.org

J.M. Roldan
Escuela Superior de Ingeniería, Universidad de Sevilla, 20134 Seville, Spain
e-mail: jmroldan@us.es

J.L. Rueda
Department of Electrical Sustainable Energy, Delft University of Technology, Mekelweg 4, 2628 CD Delft, The Netherlands
e-mail: j.l.ruedatorres@tudelft.nl

C.A. Charalambous
Department of Electrical and Computer Engineering, University of Cyprus, 75 Kallipoleos Avenue, 1678 Nicosia, Cyprus
e-mail: cchara@ucy.ac.cy

B.S. Rajpurohit
School of Computing and Electrical Engineering, Indian Institute of Technology Mandi, 175001 Mandi, Himachal Pradesh, India
e-mail: bsr@iitmandi.ac.in

for active power control, reactive power control, DC voltage regulation and AC voltage regulation. Typical MTDC consists of several VSC-HVDC terminals connected together, and different operation mode and controllers allows them interact together. DC voltage controllers play a very important role on the DC network performance. There are several DC voltage control strategies possible: voltage margin, two-stage direct voltage controller, three-stage direct voltage controller, voltage droop, etc. The contribution of this book's chapter is to present some of the main aspects regarding the modelling and simulation of two control strategies: voltage margin method (VMM) and standard voltage droop (SVD). To this end, theoretical aspects of controllers are presented and are used to develop DIgSILENT simulation language (DSL) models. The developed models are used to evaluate the performance a simple 3-terminal HVDC system.

19.1 Introduction

Electrical power systems have been developed, over more than 50 years, to deliver electricity to end-users; this approach requires using a vital infrastructure to link the energy producers and the consumers. That approach of power systems design and operation has served their purpose with great success for many decades mainly because they were developed to meet the needs of large and predominantly carbon-based energy producers located remotely from the load centres. Nowadays, power systems must cope with three driving forces of change [1]:

1. **Environmental constraints based on climate change**. The climate conference in Kyoto was the first time internationally binding targets for the reduction of greenhouse until 2012 by 5.2 % compared to 1990. The *United Nations Climate Change Conference* was held in Cancun in 2010 [2] and has agreed to continue the implementation of the Kyoto only without setting new targets for the period after 2012. However, the European Union (EU) has been seriously committed to CO_2 reduction itself. In 2007, it was agreed that the target triple of supply, competitiveness and environment should reduce the CO_2 emissions by 2020 by at least 20 % compared to 1990. Several stakeholders argue that this would not be sufficient to limit the effect of warming process of the atmosphere within 2 °C and for this reason, the EU considered to increase the reduction target to 30 % by 2020. By 2040, emissions are to be reduced by 60 %. With the use of appropriate technologies, no CO_2 should be emitted by the power generation industry by 2050 [3]. Reducing the greenhouse gas emissions by 80 % is the specific target of the UK government by 2050 [4]. This target is defined on the Climate Change Act 2008 [5]. De-carbonising the power sector is the key factor to reach this objective, and this will enable further low-carbon choices in the transport sector (e.g. plug-in hybrid and electric vehicles) and in buildings (electric heat pumps).

2. **Security of Energy Supply**. Over the coming decades, governments around the world face a daunting challenge in meeting the energy needs of a growing and developing world population while mitigating the impacts of global climate change. Security of supply is an important goal of energy policy in many countries around the world. The importance of energy security derives from the critical role that energy plays in all aspects of everyday's and business' life [6]. As demand for resources rises within today's turbulent global markets, supply chain vulnerability is becoming a significant issue. Global sourcing has created more complex and increasingly risky supply chains. Severe energy security has serious implications for social, environmental and economic well-being. The conversion of the centralised power generation structures that are currently using imported primary fuels such as coal, oil, gas and uranium to more decentralised renewable power plant systems opens the chance of reducing the import dependence from fossil energy sources. Europe as a whole is a major importer of natural gas. Apart from Norway, Russia remains one of Europe's most important natural gas suppliers. Europe's natural gas consumption is projected to grow while its own domestic natural gas production continues to decline. Increasing energy efficiency is clearly the most cost-effective part of the energy revolution. The UK's government has been working on energy security for years, making sure consumers can access the energy they need at prices that are not excessively volatile. It has been reached by a combination of its liberalised energy markets, firm regulation and extensive North Sea resources. The Department of Energy and Climate Change of UK is actively working in several aspects in order to guarantee the energy system has adequate capacity and is diverse and reliable [7].

3. **Economic development**. Development in electric power systems must contribute to growth and in parallel minimise the costs attributed to consumers. It is necessary to maintain a right balance between investing in generation, non-generation balancing technologies (i.e. storage, demand-side response and interconnection) and network assets. In addition, the efficient operation of power systems is critical to maximising the efficient use of assets across the system. When conventional power is substituted by wind power, the avoided cost depends on the degree to which wind power substitutes each of three components—fuel cost, O&M costs and capital. The economic competitiveness of wind power generation will depend on short-term prediction, and specific conditions for budding into short-term forward and spot markets at the power exchange. Some calculations demonstrate that although wind power might be more expensive than conventional power today, it may nevertheless take up a significant share in investors' power plant portfolios as a hedge against volatile fossil fuel prices [8]. Continuing research and development work is needed in order to ensure wind power is to continue reducing its generation costs and sustainable economy growth.

While current networks presently fulfil their function, they will not be sufficient to meet the future challenges described above. These challenges require technical, economic and policy developments in order to move towards lower-carbon generation technologies as well as higher efficiency devices and systems [1].

The radical changes that power systems are undergoing will change the landscape of future power networks. One of the technical challenges is the development of a Pan-European transmission network to facilitate the integration of large-scale renewable energy sources and the balancing and transportation of electricity based on underwater multi-terminal high voltage direct current (MTDC) transmission [1, 9, 10].

This kind of interconnection will facilitate markets to import and export electricity according to the market prices on either side of the interconnector using larger distances and lower losses. Increased amounts of interconnection have the potential to bring savings to the system where connected markets have different generation and/or demand profiles to trade. In such circumstances, interconnection could result in generation capacity being dispatched more efficiently and reducing the total generation capacity required. The existing power grid in Europe is a highly interconnected system, spanning the whole of Continental Europe with connections to neighbouring systems, e.g. in Scandinavia (Nordel), the UK and Russia. The current structure of this meshed, supra-national system was largely influenced by available generation technologies. The UK electricity network is connected to the systems in France (National Grid and Réseau de Transport d'Electricité, 2 GW), Northern Ireland (IFA, 2 GW) and the Netherlands (BritNed, 1GW) through "interconnectors", with others under construction or planned. Potential future interconnector opportunities include interconnectors between UK and Belgium (Nemo Link), Norway (2 GW), France, Denmark and Iceland.

Supergrid is the name of this future electricity system that will enable Europe to undertake a once-off transition to sustainability [11]. The electricity transmission system involved on supergrid should be mainly based on direct current (DC), designed to facilitate large-scale sustainable power generation in remote areas for transmission to centres of consumption, one of the fundamental attributes being the enhancement of the markets in electricity trading [12]. The North Sea has a vast amount of wind energy with largest energy per area densities located about 100–300 km of distance from shore [13]. MTDC transmission would be the more feasible solution at such distances of subsea transmission. There are several advantages of use of MTDC system, but two of those make it suitable for a massive deployment in future power systems: it allows a higher efficiency on the bulk power transmission over long distance and it provides a very high controllability in terms of power flows maximising the integration of variable power coming from renewable energy resources.

There are two kinds of HVDC transmission technology [14]: Line commutated converter (LCC)-based HVDC and voltage-sourced converter (VSC)-based HVDC. LCC-HVDC has several disadvantages [15]: it cannot perform self-restoration upon disconnection from the connected AC grid nor provide black start to the connected AC grid, in order to reverse the power transmitted; the DC voltage must be reversed. VSC-HVDC is superior to LCC-HVDC: risk of commutation failure is reduced using self-commutated switches, communication is not needed, it has black start compatibility and it has superior controllability: it is capable of independent control of active and reactive power flow.

Supergrid will probably grow in stages from connecting one offshore wind farm to one onshore grid towards linking several far offshore wind farms to multiple onshore grids [16]. It will include many HVDC cables to integrate all offshore wind power systems. When this kind of DC grid is built, connections must be made at the DC bus, multiple undersea cables and multiple converters at the same bus creating a MTDC configuration. For this, VSC-HVDC is the most appropriate technology as it uses a common DC voltage and injects a variable current [17, 18].

This book's chapter presents a discussion of the main modelling and simulation aspects of two control strategies used for MTDC: voltage margin method (VMM) and standard voltage droop (SVD). The organisation of the chapter is as follows:

Section 19.2 discusses the theoretical aspects of controllers and it is used to develop DIgSILENT simulation language (DSL) models in Sect. 19.3. Developed models are tested and validated using a simple 3-terminal HVDC system in Sect. 19.4.

19.2 Control Strategies for MTDC Network Operation

The control schemes have a large impact on system dynamics. It is an important task to determine the modelling requirements of the control schemes. The control system for a MTDC is composed of two different layers of controllers [19–22]: (i) *terminal controllers* and (ii) a *master controller* as illustrated in Fig. 19.1.

19.3 Master Controller

The *master controller* is provided with the minimum set of functions necessary for coordinated operation of the terminals in the DC circuits [20] i.e. start and stop, minimisation of losses, oscillation damping and power flow reversal, black start, AC frequency and AC voltage support. This controller optimises the overall performance
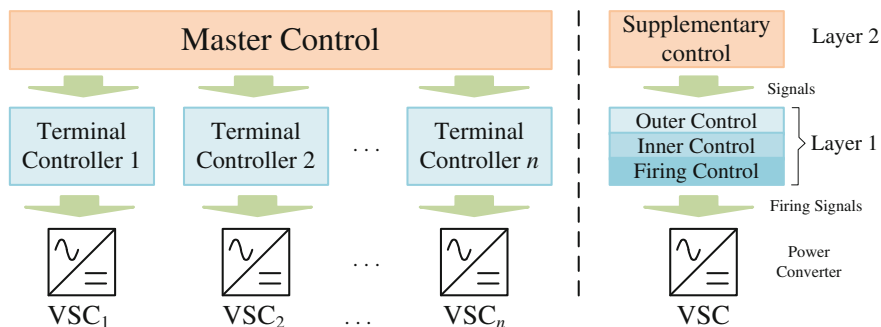

Fig. 19.1 Schematic representation of MTDC control system hierarchy

of the MTDC by regulating the DC side voltage. They are not necessary for the operation of the MTDC system, but greatly enhance their functionality.

- **Frequency control**: Frequency control is indispensable when a converter is located in a passive system, but it can also be used in an active power system. Frequency is regulated by modulating active power.
- **Damping control**: A converter can damp oscillations occurring in the AC power system by an additional controller. Input signals can be local, or not local, such as generator speeds, which may require communication. The output signal modulates active power, so that the active power swing is counteracted.
- **AC voltage control**: Instead of directly controlling AC voltage in the outer controller, an additional loop can be created around the reactive power control. The reactive power set point is determined from the desired AC voltage.

In this chapter, no models for supplementary controllers are developed. Apart from the fact that MTDC systems can operate perfectly well without supplementary controllers, the reason is that it is not desirable to come up with generic models of master controllers.

19.4 Terminal Controller

The *terminal controller* controls the specific converter by calculating the pulse-width modulation (PWM) pulses for the converter bridges. The firing controller is the fastest controller and inner control, outer control and supplementary control are used for increasingly higher level functions and have increasingly higher cycle times. This MTDC control system is implemented on a hierarchical way. It is a cascaded system, where every level accepts the input of the previous one and feeds its output signal to the next level. This is schematically represented in Fig. 19.1.

19.5 Firing Control

Firing control is the lowest control level inside the terminal control system and it acts very fast. Firing control, also known as valve control, takes the desired converter waveform as an input and determines by means of the valve firing logic the pulses that need to be generated [23]. The firing logic is communicated to the controllable switches (e.g. IGBTs GTO's), and pulses are generated that switch on/off the switched at the appropriate instants. The firing instances are synchronised using a phase-locked loop (PLL).

The pattern of the pulses depends on the topology of the bridge and the switching method. As converters are considered to be a black box, the details of the converter topology are not known and modelling the firing control is impossible. However, firing control has cycle times in the few micro-seconds range. The use of

Fig. 19.2 Equivalent circuits in d and q axes of VSC-HVDC for d-axis aligned with voltage phasor of phase-a
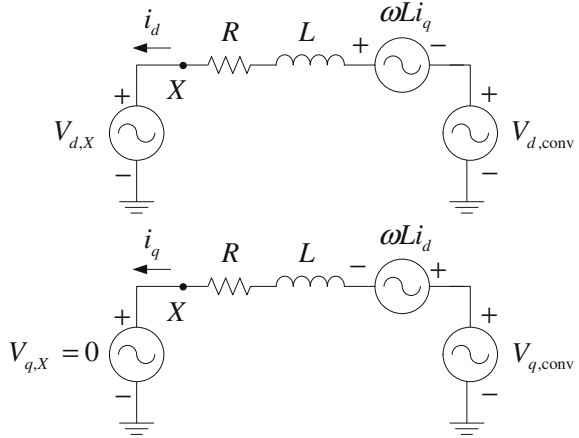
the *space vector* in the control design and implementation enables to make a fully decoupled linear control of active and reactive currents.

The d-q reference frame is selected in such a way that the d-axis is aligned to the voltage phasor of phase-a of point X. This means that the PLL should be phase locked to phase-a voltage phasor of the reference point, X. This results in

$$V_{q,X} = 0$$
$$V_{d,X} = V_X \qquad (19.1)$$

The simplified equivalent model of VSC-HVDC in d-q reference is shown in Fig. 19.2. From the d-q equivalent circuit as observing from the reference point X, the apparent power (S_{conv}) injected by the VSC converter into the AC network is given by:

$$S_{\text{conv}} = \frac{1}{2}\left(V_{d,X} + j0\right)\left(i_d - ji_q\right) \qquad (19.2)$$

The active and reactive powers (P_{dq}, Q_{dq}) provided by the VSC-HVDC converter to the AC become:

$$P_{dq} = \frac{3}{2}V_{d,X}i_d \qquad (19.3)$$

$$Q_{dq} = -\frac{3}{2}V_{d,X}i_q \qquad (19.4)$$

19.6 Inner Controller

The *inner control or current control loop* is designed to be much faster than the outer controllers. It is not fast enough, however, to warrant neglecting its dynamics. This means current controllers and all relevant controllers higher in the hierarchy must be modelled. This control system controls the current through the phase reactor. Decoupled control is used, which means that voltages and currents are decomposed in *dq*-components, controlled independently [23]. The output of the current control is the desired converter voltage.

The inner current controller is developed based on the following equation.

$$L\frac{d}{dt}\begin{bmatrix} i_d \\ i_q \end{bmatrix} = \begin{bmatrix} V_{d,X} \\ V_{q,X} \end{bmatrix} - \begin{bmatrix} V_{d,\text{conv}} \\ V_{q,\text{conv}} \end{bmatrix} - r\begin{bmatrix} i_d \\ i_q \end{bmatrix} - \omega L\begin{bmatrix} 0 & 1 \\ -1 & 0 \end{bmatrix}\begin{bmatrix} i_d \\ i_q \end{bmatrix} \quad (19.5)$$

An implementation of Eq. (19.5) is presented in Fig. 19.3, and it shows the *d*- and *q*-components of current controllers of the inner current loop.

The power converter has a time delay caused by the sinusoidal pulse-width modulator and it can be approximated as:

$$e^{-T_w s} \approx \frac{1}{(1 + T_w s)} \quad (19.6)$$

where time delay is defined by $T_w = 1/2 f_s$, where f_s is the switching frequency of the converter. Proportional integral (PI) controllers are used for closed loop control and the zeroes of the PI controllers are selected to cancel the dominant pole in the external circuit [13]. The time constant $\tau = L/r$ is much higher than T_w for a typical VSC, and hence will be the dominant pole to be cancelled. The cross-coupling currents in Eq. (19.4) are compensated by feed-forward terms in the controllers as shown in Fig. 19.3.
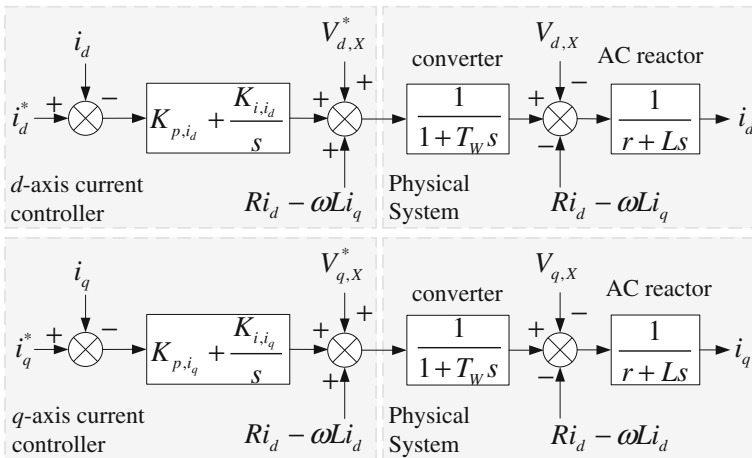

Fig. 19.3 Inner current controllers

19.7 Outer Controller

The *outer controllers* are the ones responsible for providing the current references signals for the inner current controller. The terminal controller determines the behaviour of the converter at the system bus. Several targets can be set [4, 12]:

- **Active power control**: determines the active power exchanged with the AC grid.
- **Reactive power control**: determines the reactive power exchanged with the AC grid.
- **AC voltage control**: instead of controlling reactive power, AC voltage can be directly controlled, determining the voltage of the system bus.
- **DC voltage control**: used to keep the DC voltage control constant.

The outer controllers have in common their provision of a current set point in the *dq*-frame for the inner current controller. Their behaviour directly influences the dynamics of the AC system and are therefore of paramount importance in modelling MTDC systems.

Active current (i_d) is used to control either of active power flow or DC voltage level. Similarly, the reactive current (i_q) is used to control either of reactive power flow into stiff grid connection or AC voltage support in weak grid connection.

19.7.1 Active Power Controller

The active power flow (P) of the VSC-HVDC terminal is given by Eq. (19.3):

$$P_{\mathrm{dq}} = \frac{3}{2} V_{d,X} i_d \qquad (19.3)$$

where V_x is resultant voltage in *dq*-reference frame and is desired to have a constant value. Hence, active power flow can be controlled by active current (i_d).

This controller allows an excellent control on the active power exchanged with the AC grid. An implementation of the active power controller is presented in Fig. 19.4a.

The output of the active power controller (i_d^*) provides the reference input to the *d*-axis current controller of the inner current loop in Fig. 19.3. The maximum current through the VSC-HVDC converter must be controlled in order to avoid potentially dangerous over currents on the commutation devices. In order to limit the magnitude of current in the VSC-HVDC to a maximum limit, the output of the active power controller is followed by a limiter function of $\pm I_{\max}$ limits, where:

$$-I_{\max} \leq i_d^* \leq +I_{\max} \qquad (19.7)$$

where $I_{\max} = I_{\mathrm{rated}}$.

Fig. 19.4 Outer controllers
a Controllers PI controller for
active power control.
b Controllers PI controller for
reactive power control.
c Basic scheme for AC
voltage controller
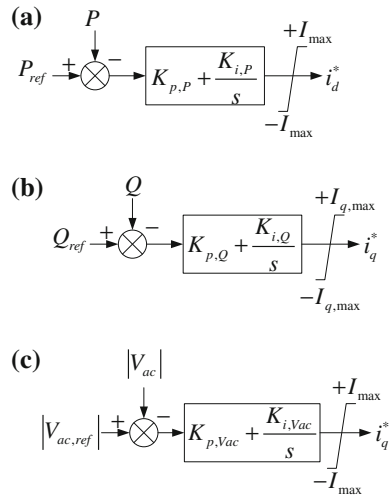
19.7.2 Reactive Power Controller

The reactive power (Q) exchanged by the VSC-HVDC converter and the AC grid is given by Eq. (19.4):

$$Q_{dq} = -\frac{3}{2} V_{d,X} i_q \qquad (19.4)$$

The reference of reactive current (i_d^*) is used to control the reactive power flow provided by the VSC-HVDC converter and an implementation of this controller is presented on Fig. 19.4b. As in the case for active power control, i_q* will be the reference input for the reactive current controller of the inner current loop in Fig. 19.3.

The reference of reactive current (i_d^*) must be limited in order to avoid any damage on the commutation devices; as a consequence, i_d^* is limited to $\pm I_{q,max}$ in such a way that the total converter current should not exceed the rated current ($I_{max} = I_{rated}$). This takes the assumption that that priority is given to the transfer of active power. Hence:

$$I_{q,max} = \sqrt{I_{max}^2 - \left(i_d^*\right)^2} \qquad (19.8)$$

19.7.3 AC Voltage Controller

A VSC-HVDC converter connected to a power system has the capability to control the AC voltage at the connection point; this feature is especially important on a weak grid, where there is significant line resistance and inductance creating a considerable amount of voltage fluctuations with changing active power flow.

This controller is designed to regulate the amplitude of the AC voltage (V_{ac}) at the common bus to be equal to the given reference value by modifying i_d^*. This implies that the controller governs the converter to generate an amount of reactive power so that the voltage at the common bus matches the given reference value ($V_{ac,ref}$). An implementation of this controller is presented on Fig. 19.4c.

19.8 DC Voltage Controller

DC voltage control is certainly one of the most important tasks given to the VSC-HVDC stations inside a MTDC network. A well-controlled DC voltage on a MTDC system is a guarantee of the power balance between all the interconnected nodes. Considering the operational requirements for DC voltage on MTDC, the literature provides two main control strategies which possibly can be applied in future transnational networks [24]: (i) the *direct voltage droop method* and the (ii) *voltage margin method*. These methods enable sharing of load among two or more DC voltage regulating terminals operating in parallel and provide controls in MTDC. Figure 19.7 shows a general scheme for VSC-HVDC system considering only two converter substations (Fig. 19.5).

19.8.1 Principle of Voltage Margin Method (VMM)

The *voltage margin* is defined as the difference between the DC reference voltages of the two terminals (ΔU_{dc}) [20]. Figure 19.6a shows the $U_{dc}-P$ characteristics of both terminals at Terminal A, and the intersection $U_{dc}-P$ of the characteristics of each terminal is the operating point "a".

When the active power is to be transmitted from Terminal B to Terminal A ($P_A < 0$, $P_B > 0$), the voltage margin (ΔU_{dc}) is subtracted from the DC reference voltage for Terminal A. Terminal B (rectifier) determines the DC system voltage
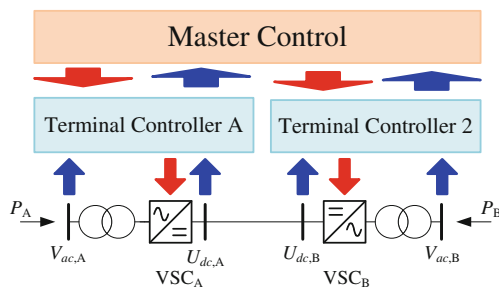

Fig. 19.5 General scheme for two converter stations VSC-HVDC system. VSC$_i$ operates as inverter ($P_i < 0$) or rectifier ($P_i > 0$) depending in power direction
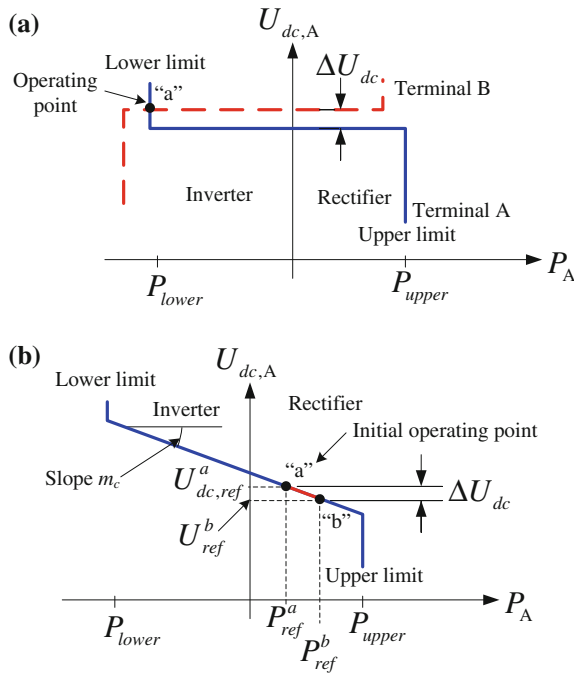
(a)

(b)

Fig. 19.6 $U_{dc}-P$ characteristics of DC voltage controllers. **a** $U_{dc}-P$ characteristic showing the operating point "a" in VMM for one terminal **b** $U_{dc}-P$ characteristic showing the operating point "a" in VMM for one terminal

and Terminal A (inverter) controls the active power (P_A) determined by the lower limit of the DC voltage regulator. The DC voltage controller tries to keep the DC voltage to the reference value $U_{dc,ref}$ by adjusting P_A, until P_A reaches the upper limit or the lower limit (see Fig. 19.7).

The VMM gives reliable way of controlling MTDC without the need for communication between terminals and is capable of keeping the steady-state voltage with in pre-set limits even after load switching and disconnection of some converter terminals. But on the other hand, this method implies allocation of only one terminal at a time for the regulation of DC voltage and the other terminals do not experience significant change during changes in power flow of the DC network.

Fig. 19.7 Basic scheme for VMM controller with adjustable limits
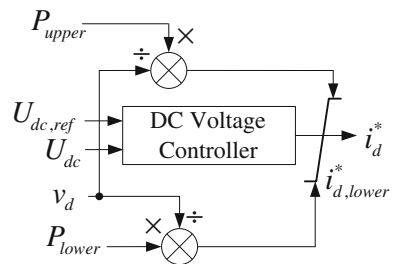
19.8.2 Principle of Voltage Droop Method (VDM)

Frequency droop control is a well-established method and the basis for stable operation in all AC grids. The system's frequency is used as a global measure for the instantaneous balance between power generation and demand [25]. The *DC voltage droop method* is a coordinated control to maintain a power balance and a desired power exchange in the MTDC. This control is a modification of the *VMM* control where the horizontal line sections ($P_{lower} < P_A < P_{upper}$) of the U_{dc}–P characteristic curves is replaced by a line with small slope (m_c) [26]. The DC voltage droop, m_c, indicates the degree of compensation of power unbalance in the DC grid at a cost of reduction in the DC bus voltage. This principle of *VMM* control is shown in Fig. 19.6b. When $U_{dc,A}$ drops (e.g. due to large withdrawal of power someplace else in the DC network, operation point moves from "a" to "b"), the slack converter station (VSC$_A$) will increase the active power injection in the DC grid P_A until a new equilibrium point ($U_{dc,ref}^b, P_{A, ref}^b$), at a lower DC voltage, is reached ($U_{dc,ref}^b = U_{dc,ref}^a - \Delta U_{dc}$). The use of a proportional DC voltage controller allows multiple converters to regulate the voltage at the same time and the concept of distributed slack bus is possible.

Figure 19.8 shows how the droop characteristic is implemented based on the power active controller. When the voltage droop control is used in the absence of a PI controller, the voltage controller's active power P will change when the value of the DC bus voltage changes.

19.9 Dynamic Modelling in DIgSILENT Power Factory

DIgSILENT PowerFactory has developed highly flexible and accurate features for time-domain modelling. The DSL provided to PowerFactory the capability to define new dynamic controllers which receive input signals from the simulated power system and subsequently react by changing some other signals. DSL itself can be looked upon as an add-on to the transient analysis functionality of PowerFactory. The DSL language is used to programme models for the electrical controllers and other components used in electrical power systems.
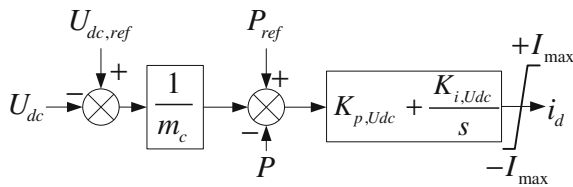

Fig. 19.8 Voltage droop controller

This simulation tool falls into the category of continuous system simulation language (CSSL), originally designed by the Simulations Council Inc (SCI) in 1967 in an attempt to unify the continuous simulations field. This programming approach allows the modelling and simulation of systems characterised by ordinary and partial differential equations.

DSL allows the definition of every linear or nonlinear system of differential equations, dead times (e.g. ideal wave equations), arithmetic or logic expression (e.g. digital controllers), and event (e.g. open breaker if $x > y$).

PowerFactory uses a *partitioned solution* with *explicit integration* method on the solution of the differential algebraic model (DAE) for power system dynamic analysis. During the time-domain simulation, the model equations of the DSL models are combined with those describing the dynamic behaviour of the power system components. These equations are then evaluated together, leading to an integrated transient simulation of the combination of the power system and its controllers.

PowerFactory modelling philosophy is targeted towards a strictly *hierarchical system modelling approach* as depicted in Fig. 19.9.

DSL is a very flexible language and it can be used for: (i) writing a DSL-programme, (ii) drawing a block diagram, or (iii) combination of both approaches. In this book's chapter, a combination of drawing a block diagram and writing DSL-commands is used. Creating a general methodology to develop dynamic models using DSL is beyond the scope of this chapter, however, a simple 3-step procedure can be followed as general rule: *Step* 1: Create the Frame Diagram showing how the slots are interconnected, *Step* 2: Create each of the model definitions and set appropriate initial conditions, *Step* 3: Create a composite model and fill the slots with the relevant elements. The development of those steps on the case of inner and outer controller of a MTDC system is shown in the next sections.

19.10 Modelling a MTDC in DIgSILENT Power Factory

One of the main components on a MTDC system is the VSC-HVDC power converter. A PWM converter model (*ElmVscmono*) is used for VSC-HVDC converter stations; it represents a self-commutated, voltage source AC/DC converter (with a capacitive DC-circuit included). This built-in model (*ElmVscmono*) is shipped by default without any controls, for this reason DSL model for controllers must be
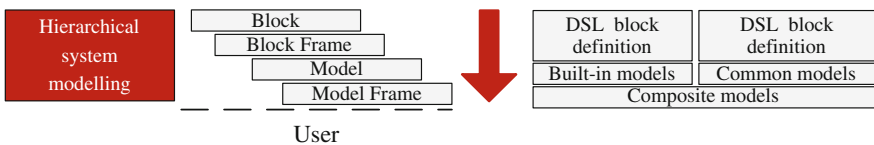

Fig. 19.9 Schematic representation of the DSL hierarchical system modelling approach

developed. A set of four input variables can be defined of the PWM converter model. It allows specifying a pulse-width modulation index-vector, with reference to a reference-system that is defined by *cosref* and *sinref*. *Pmr* and *Pmi* are the real and imaginary components of pulse-width modulation index based on the output of a *dq*-current controller.

The MTDC system is expected to consist of several VSC-HVDC terminals connected to each other through the DC network. Local control at each terminal should be able to adopt a control strategy depending on the specific needs described by the basic features required by MTDC system. The terminal controller must monitor DC and AC side and should control DC side parameters as well as AC side parameters. Using the bus parameter control on DC and AC side, several operation modes can be defined, a discussion about the all possible different control modes of VSC-HVDC terminal can be found in [13].

Two reactive power control functions are included into VSC-HVDC stations from the AC network side [15]: (i) *Q*-mode: the reactive power injected ($Q_{ac,i}$) into the AC network is kept constant, as consequence the AC voltage ($V_{ac,i}$) might change. (ii) *V-mode*: the reactive power converter injection ($Q_{ac,i}$) is enough to keep is AC node voltage magnitude ($V_{ac,i}$) constant. On the DC network side, there are two different control functions for each converter: (i) P_{ac}-control: The active power ($P_{ac,i}$) injected in the AC network is kept constant and the AC voltage ($V_{ac,i}$) is allowed to vary, (ii) U_{dc}-control: The converter controls its active power injection ($P_{ac,i}$) to keep its DC node voltage constant ($U_{dc,i}$).

Consider the schematic representation of the MTDC control system's hierarchy which is shown in Fig. 19.1. This section deals with the implementation of the inner and outer controller as presented in Sect. 19.2. Next sections show the DSL implementation of outer controllers for a MTDC system. The implementation presented in this chapter considers two possible operation modes for the terminals controllers: *PQ*-control and *Q*-U_{dc}-control. The components of pulse-width modulation index (*Pmi* and *Pmr*) are calculated using a *dq*-current controller.

19.10.1 Composite Frame

The composite model provides an overview diagram showing the interconnections between slots. Each block on those frames (slots) is placeholders for the models that describe their dynamic behaviour. A composites frame is a block definition object (*BlkDef*) which contains only slots and connectors, showing how the network elements and common models are connected together. Figure 19.10a and b shows the composite frame for *PQ*-control and *Q*-U_{dc}-control, respectively. Those composite frames contain the definitions of each slot, indicating the type of object assigned to the slot.

The composite frame for *PQ*-control consists of several slots: active and reactive measurement blocks, PLL measure system, model for active power control (*P*-controller), model of reactive power control (*Q*-controller), model of frequency
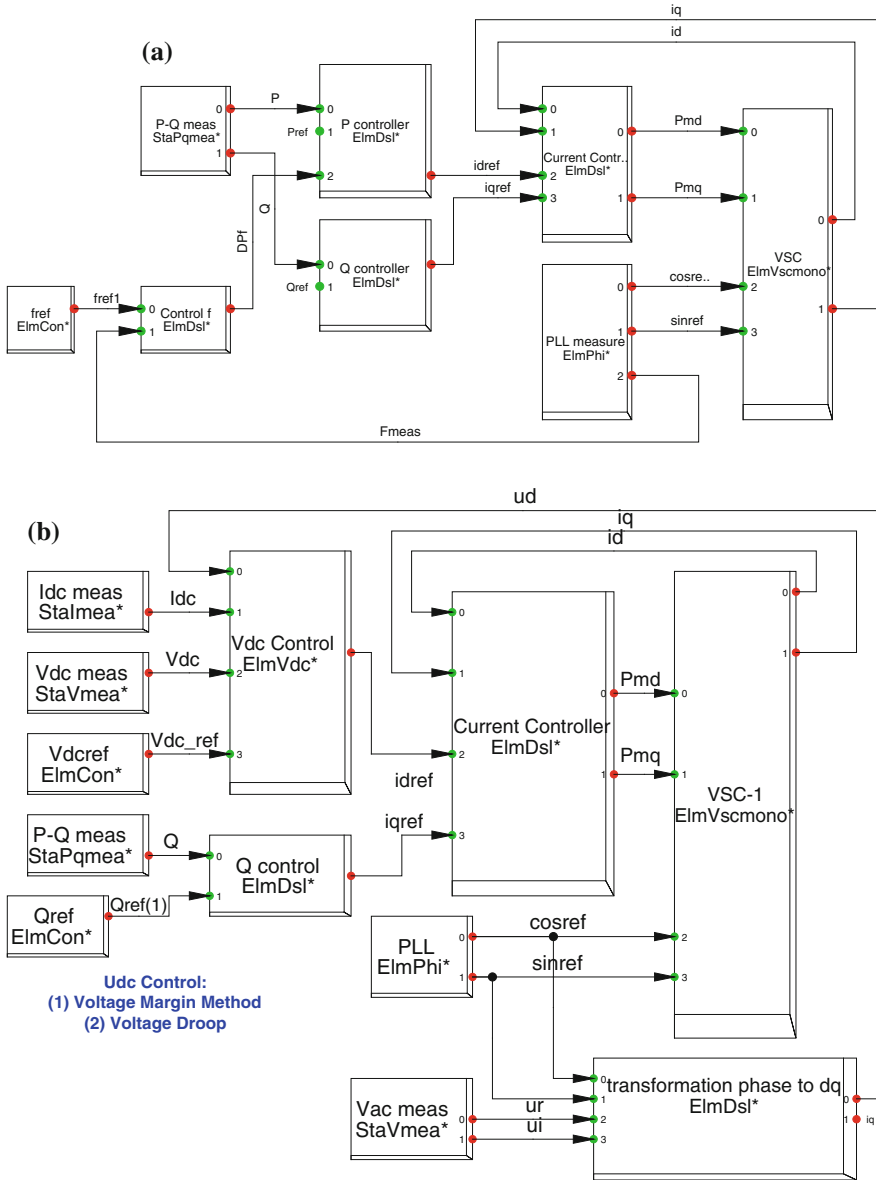
Fig. 19.10 Composite frames of terminal controllers in MTDC system. **a** Composite frame for *PQ*-control. **b** Composite frame for *Q-U*dc-control

control (Control *f*), *dq*-current control frame (Current Controller) and finally the modulation indexes (*Pmd* and *Pmq*) which are fed into the power converter (*ElmVscmono*). The composite frame for *Q*-U_{dc}-control consists of several slots: active and reactive measurement blocks, PLL measure system, DC current and voltage measurements, AC voltage measurements, model for reactive power control (*Q*-controller), model DC voltage control (Vdc controller), *dq*-transformation used for the AC voltage, *dq*-current control frame (Current Controller) and finally the modulation indexes (*Pmd* and *Pmq*) which are fed into the power converter (*ElmVscmono*).

19.10.2 Model Definitions

The model that describes the dynamic behaviour of each controller on the frames must be defined by a block diagram, called in DSL as *model definition*. This defines the transfer function of a dynamic model, in the form of equations and/or graphical block diagrams. Figure 19.11 shows the model definitions created based on the controllers presented in Fig. 19.4a, b for active and reactive power controllers. A limited first-order transfer function $\{K\,(1 + 1/sT)\}$ is used to model the PI block. This is an equivalent version of the classical PI transfer function ($k_p + k_i/s$) where $k_p = K$ and $k_i = K/T$.

The *dq*-current controller used in the DSL implementation of the inner controller is a slightly different version of the block diagram presented in Fig. 19.3.
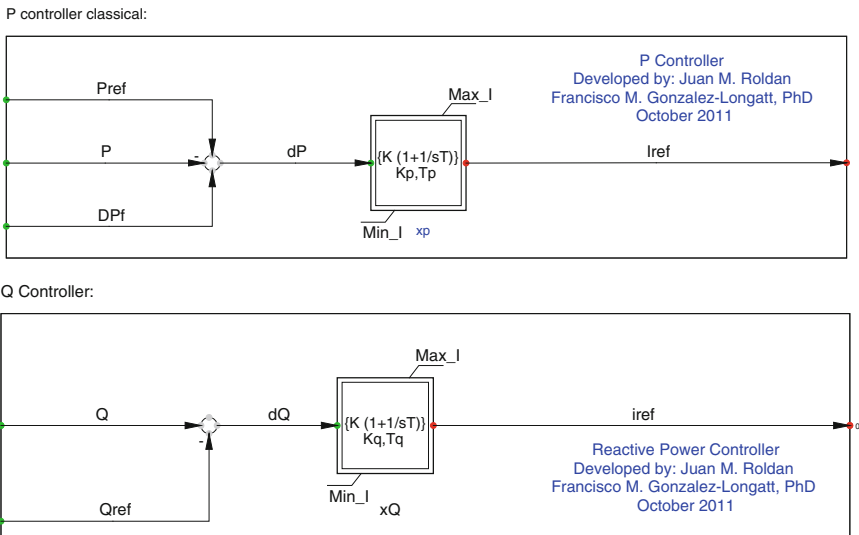

Fig. 19.11 Model definition for active and reactive power controllers

The DC voltage controllers are depicted in Fig. 19.13. A limited proportional integral function $\{K(1 + 1/sT)\}$ is used on the model definition and the DC control method for DC VMM and droop controller are presented in Fig. 19.13a, b, respectively.

19.10.3 Model Initialization

All DSL models must be initialized according to the steady-state conditions. In PowerFactory, the steady-state conditions are obtained from the load flow calculations (*ComLfd*) prior to a time-domain simulation. New user-defined DSL models require a proper initialization in order to reach correct results in time-domain simulations. In a DSL model, all variables or signals that cannot be determined directly from the load flow solution must be manually initialised. However, it must be noticed, not all variables and signals in a model need to be manually initialised. PowerFactory will try to use the model equations to compute its initial value. However, the classical error message will appear if the model equations have undefined variables or signals (e.g. an unknown input). The initialization process typically starts from the grid elements and goes backwards through the other models, fully initializing each block at a time.

The best procedure for composite block initialization is as follows: *Step* 1: clearly define the signals flow, *Step* 2: determine which signals or variables are known and unknown, *Step* 3: use the final value theorem (FVT) to calculate output steady-state of common primitive blocks. An alternative method to FVT is using the state-state model representation and set all derivative terms to zero. *Step* 4: calculate the unknown signals (and variables) in terms of the known quantities.

The developed DSL model of the MTDC in this chapter in DIgSILENT Power Factory requires two composite frames and at least seven model definitions. A detailed illustrative example of model initialisation is presented in this chapter for space constraints.

The active power controller presented in Fig. 19.11a is based on limited proportional integral function $\{K(1 + 1/sT)\}$ which is already built-in the global library for macros in PowerFactory using a DSL model where the state variable is *x*. The DSL code representation for the built-in model of this function in terms of dynamic equations is as follows:

```
b1 = K/T                                         ! Constant definition
x. = yi                                          ! State variable equation
yo=lim(b1*limstate(x,Ymin/b1,Ymax/b1)+K*yi,Ymin,Ymax)  ! yo Limit
limits(T)=(0,]                                   ! safety check
```

The initialization of this common primitive block is very simple. In steady state, the derivative terms are zero and there is nothing to integrate, as a consequence, the

input $yi = 0$. The output is already at its steady-state value $y_o = y_{o,ss}$, which is known or calculated from the steady-state values obtained from the load flow quantities.

The state variable, x, must be initialized to the steady-state output $y_{o,ss}$. Now, this initialization must be implemented in the block definition of the model of P-controller. The DSL implementation of active power controller has three inputs: *DPf*: changes on active power caused by frequency, *P*ref: reference of active power and *P*: actual active power obtained from circuit measurement. The active power in the MTDC system is obtained from the steady-state conditions obtained from the load flow calculation, as consequence the reference of this controller is initialized at such value, (*Pref = P*). The system frequency in steady state is equal to the nominal frequency, and there are no changes on the active power caused by frequency deviation; as a consequence, the changes on active power caused by frequency must be initialized at zero (*DPf = 0*). DSL code representation for the model initialization is as follows:

```
1: inc(DPf) = 0                              ! P changes cased by f
2: inc(Pref) = P                             ! P reference
3: inc(xP) = idref*Tp/Kp                     ! State variable, named xP
4:
5: ! Variable Definition
6: vardef(Kp) = 'p.u.'; 'P Controller Gain'
7: ardef(Tp) = 'sec'; 'P Controller Time constant'
8: vardef(Min_I) = 'p.u.'; 'Min d-q axis I'
9: vardef(Max_I) = 'p.u.'; 'Max d-q axis I'
```

The same procedure for initialization is followed for the *Q*-controller shown in Fig. 19.11b, and DSL code for the model initialization is as follows:

```
1: inc(Qref) = Q                             ! Q reference
2: inc(xQ) = idref*Tq/Kq                     ! State variable, named xQ
3: ! Variable Definition
4: vardef(Kq) = 'p.u.'; 'Q Controller Gain'
5: vardef(Tq) = 'sec'; 'Q Controller Time constant'
6: vardef(Min_I) = 'p.u.'; 'Min d-q axis I'
7: vardef(Max_I) = 'p.u.'; 'Max d-q axis I'
```

DSL code for the model initialization of the dq-current controller is shown in Fig. 19.12.

```
inc(xq)=Pmq*T/K                              ! State variable, named xq
inc(xd)=Pmd*T/K                              ! State variable, named xd
inc(idref)=id                                ! d-axis current reference
inc(iqref)=iq                                ! q-axis current reference
! Variable Definition
vardef(T)='s';'dq-axis Current Measurement Time Constant'
vardef(K)='p.u.';'dq-axis Gain'
vardef(Min_Pm)='p.u.';'Min. dq-axis modulation index'
vardef(Max_Pm)='p.u.';'Max. dq-axis modulation index'
vardef(Max)='p.u.';'Max. modulation index'
vardef(Max_I)='p.u.';'Max. module current'
```
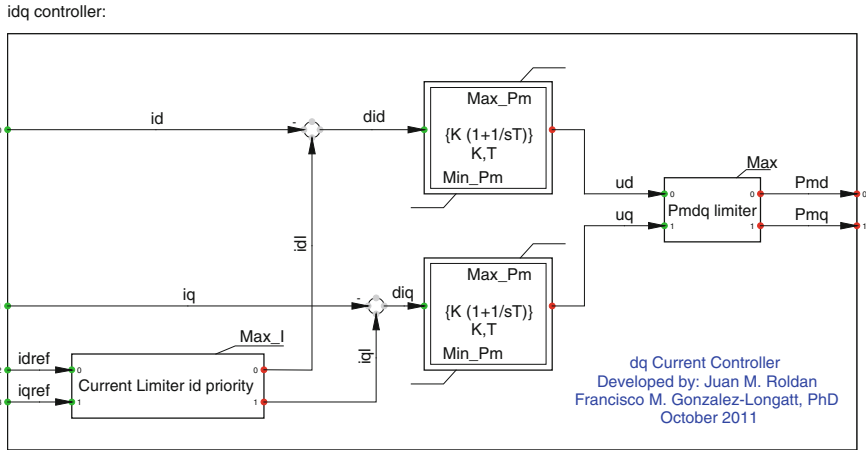
idq controller:

Fig. 19.12 Model definition for dq-current controllers

Finally, the DSL codes for the model initialization of the DC voltage controllers are presented in (Fig. 19.13):

```
! Voltage Margin Method: Model initialization
inc(o1)=idref-(Vdc/ud)*2*Idc/3              ! State variable, named o1
inc(xu)=o1*Tu/Ku                            ! State variable, named xu
inc(Vdc_ref)=Vdc                            ! Reference of DC voltage
inc(Pref)=P                                 ! Reference of active power
inc(xP)=idref*Tp/Kp                         ! State variable, named xP
! Variable Definition
vardef(Kp)='p.u.';'P Controller Gain'
vardef(Tp)='p.u.';'P Controller Time Constant'
vardef(Ku)='p.u.';'Controller Gain u'
vardef(Tu)='sec';'Controller Time Constant u'
vardef(Min_I)='p.u.';'Min. q-d axis I'
vardef(Max_I)='p.u.';'Max. q-d axis I'
```

```
! Voltage Droop Method: Model initialization
inc(Pref)=P
inc(Vdcref)=Vdc
inc(xP)=idref*Tp/Kp
! Variable Definition
vardef(Kv)='p.u.';'P-V slope (negative)'
vardef(Kp)='p.u.';'P Controller Gain'
vardef(Tp)='p.u.';'P Controller Time Constant'
vardef(Min_I)='p.u.';'Min. q-d axis I'
vardef(Max_I)='p.u.';'Max. q-d axis I'
```
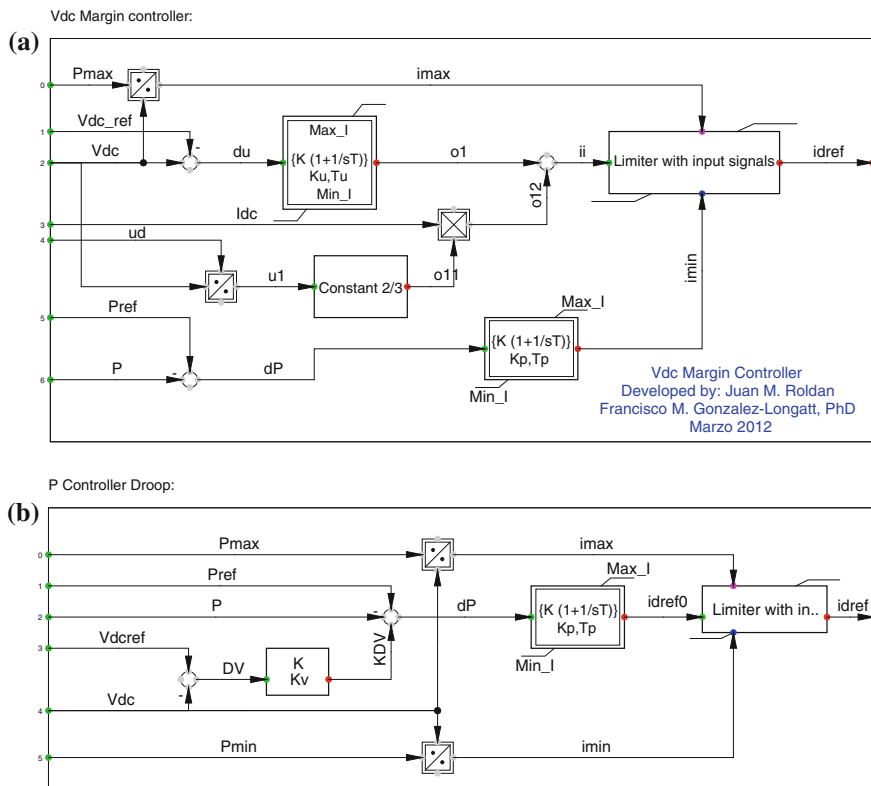
Vdc Margin controller:

P Controller Droop:

Fig. 19.13 Model definition of DC voltage controllers. **a** DC voltage margin controller method. **b** DC voltage droop controller method

19.11 Application Example

In this Section, the dynamic behaviour of the implementation of a MTDC system in DIgSILENT PowerFactory is demonstrated. Time-domain simulations on a AC/DC test system are used to analyse the performance of the controller following a converter outage when considering two DC voltage control strategies: VMM and voltage droop method. The test network used in this paper is the classical 5-bus test network which is taken from G.W. Stagg and A.H. El-Abiad [27] and 3-node VSC-MTDC network with is connected to the AC test system (Fig. 19.14).

The converter at bus 3 (VSC37) is chosen as a DC slack bus, thereby controlling the voltage on the DC network. This converter station is also used to control the voltage at bus 3 and it is the main target to evaluate two different DC voltage control strategies. The other converter stations (VSC26 and VSC58) are directly controlling their reactive power injections (constant Q-mode). Data on the converter station phase reactors and line resistances can be obtained from [14, 28].
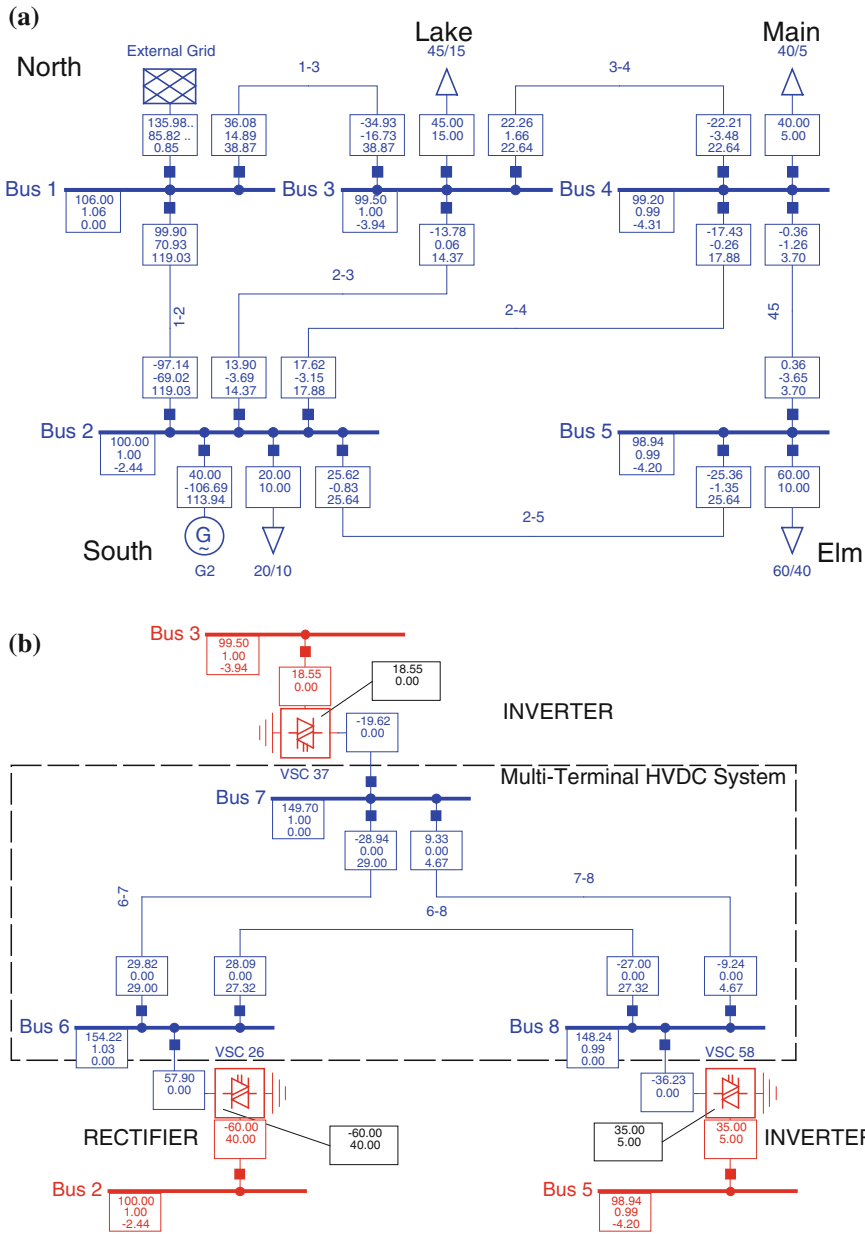
(a)

(b)

Fig. 19.14 AC/DC test system **a** AC test system: 5-node AC network. **b** DC test system: 3-node VSC-MTDC system

19.11.1 Case I: Sudden Load Increase

A sudden load increase of 40 MW on bus 3 is considered in this scenario. The dynamic behaviour of DC voltage at bus 6 and AC bus 5 is depicted in Fig. 19.15a and b.

The blue line shows the bus voltage's response having only one voltage controller operating, VMM. The red line represents the dynamic response when a voltage droop controller ($m_c = -0.1$) is operating on converter station VSC26. The transient over-voltages and under-voltages are reduced as expected using the droop control. The slopes of the voltage droop controller considered in this simulation are $1/m_c = -10.0$, -8.0 and -2.0 p.u. for converters VSC26, VSC37 and VSC58, respectively.

19.11.2 Case II: One Converter Outage

This simulation results are used to investigate the effect of a distributed voltage droop control on bus 2 (VSC26). Two different values of voltage droop slope (m_c) have been tested. Result shows the dynamic response of bus voltages is clearly influenced by the voltage droop characteristic. Figure 19.16a shows response of bus voltage at bus 6 considering a perturbation based on the outage of VSC58.

Fig. 19.15 Dynamic response of V_{ac} at Bus 5 (*bottom*) and U_{dc} at Bus 6 (*top*) after sudden load increase event considering two control strategies: voltage margin (*blue*) and droop (*red*). Case I. **a** Bus 6. **b** Bus 5
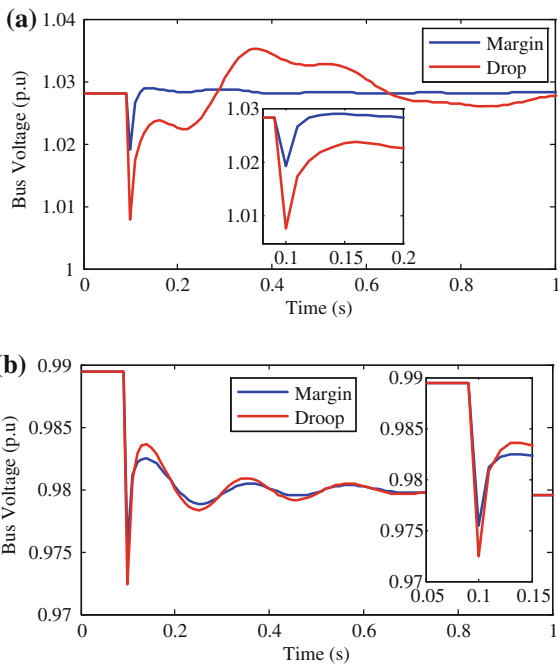
As shown, an incorrect selection slope value may causes transient responses with greater over-voltages on the DC bus (Droop B, green line). However, if voltage droop slope is appropriately selected, it can mainly assist the voltage at slack bus 3 and the system can handle transients caused by one converter station outage.

The AC voltage transient response is not significantly influenced by the voltage droop slope as shown in Fig. 19.16b. When the droop control is implemented in a larger DC network, the contribution of each converter to the DC voltage control can be adapted by modifying its droop characteristic. The values of the voltage droop slope used in this simulation are shown in Table 19.1.

Regarding the power load flow, the slack station-converter at bus 3 (VSC37) adapts its power, whereas the power injected by the converter at bus 2 (VSC26) remains unaltered. After a sudden converter-station disconnection, bus voltage at the remaining converter in operation exhibits a voltage droop which is previously defined by the Droop B characteristic. As shown by the results, the remaining converter powers are both lowered, dictated by their droop characteristics. Simulation shows the voltage margin control is capable to survive a converter outage just if this converter is operating on constant power mode.

Different values of voltage droop slope have been tested showing that the transient response is clearly influenced by the voltage droop characteristic. When two converters on the MTDC operate with DC voltage droop characteristic, it

Fig. 19.16 Dynamic response on case II. a Bus 6, DC voltage transient with margin and droop control strategies. b Bus 5, AC voltage transient with margin and droop control strategies
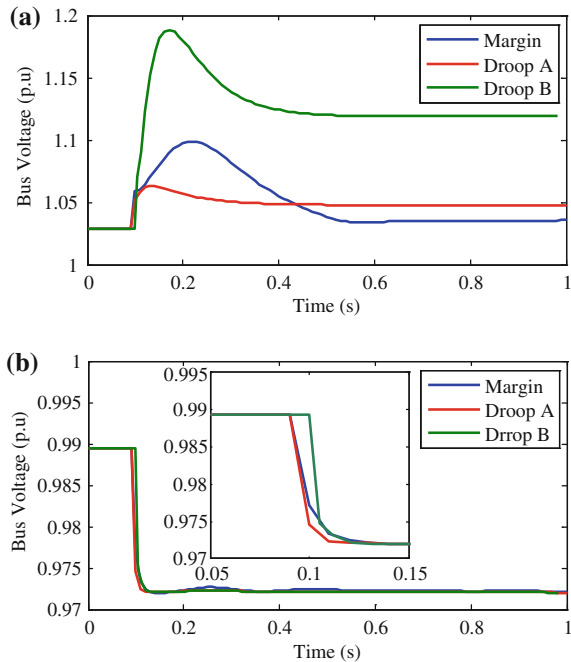
Table 19.1 Slope of voltage droop characteristic (p.u.)

Droop A $(-1/m_{c,i})$		Droop B $(-1/m_{c,i})$	
VSC23	VSC37	VSC23	VSC37
−10.0	−8.0	−2.0	−2.0

appears a "collaborative scheme" for the DC voltage support, sharing the task of controlling the DC voltage. Simulation results demonstrate the voltage margin control is capable to survive a converter outage just if this converter is operating on constant power mode.

References

1. Gonzalez-Longatt F (2014) Frequency Control and Inertial Response Schemes for the Future Power Networks. In: Hossain J, Mahmud A (eds) Advances in technologies for generation, transmission and storage, green energy and technology series, vol VIII. Springer, Singapore, p 363
2. UN (2011) The conference of the parties (15 Mar 2011). The Cancun agreement. FCCC/CP/2010/7/Add.1, Decision 1/CP.16, The Cancun agreements: outcome of the work of the Ad Hoc working group on long-term cooperative action under the convention. Decision (1/CP.16). Available from http://unfccc.int/resource/docs/2010/cop16/eng/07a01.pdf
3. EUREL Electrical Power Vision 2040 for Europe (Online). Available from www.eurel.org/home/…/EUREL-PV2040-Full_Version_Web.pdf
4. GOV. UK (2011) Policy reducing the UK's greenhouse gas emissions by 80 % by 2050. Available from https://www.gov.uk/government/policies/reducing-the-uk-s-greenhouse-gas-emissions-by-80-by-2050
5. legislation. gov. UK (2008) Climate Change Act 2008. Available from http://www.legislation.gov.uk/ukpga/2008/27/contents
6. Winzer C (2012) Conceptualizing energy security, Energy Policy, 46:36–48
7. DECC (2013) Department of energy and climate change. Available from https://www.gov.uk/government/organisations/department-of-energy-climate-change
8. EWEA (2011) European wind energy association: policy/project—offshore wind. Available from http://www.ewea.org/index.php?id=203
9. Cornago AA (2011) Can the European supergrid become reality? Available from http://www.publicserviceeurope.com/article/406/can-the-european-supergrid-become-reality
10. Chauhan RK, Rajpurohit BS, Singh SN, Gonzalez-Longatt FM (2014) DC grid interconnection for conversion losses and cost optimization. In: Mahmud A, Hossain J (eds) Renewable energy integration. Springer, Singapore, pp 327–345
11. FOSG (2011) Friends of the Supergrid. Available from http://www.friendsofthesupergrid.eu/
12. FOSG (2010) Friends of Supergrind. Position paper on the EC Communication for a European Infrastructure Package. Available from http://www.friendsofthesupergrid.eu/documentation.aspx
13. Haileselassie TM (2008) Control of multi-terminal VSC-HVDC systems, master of science in energy and environment. Department of Electrical Power Engineering, Norwegian University of Science and Technology, Trondheim
14. Gonzalez-Longatt F, Roldan J (2012) Effects of DC voltage control strategies of voltage response on multi-terminal HVDC following a disturbance. In: 47th International Universities Power Engineering Conference (UPEC 2012), pp 1–6

15. Gonzalez-Longatt F, Roldan J, Charalambous CA (2012) Power flow solution on multi-terminal HVDC systems: supergrid case. Presented at the international conference on renewable energies and power quality (ICREPQ'12), Santiago de Compostela
16. Vrana TK, Torres-Olguin RE, Liu B, Haileselassie TM (2010) The North Sea super grid—a technical perspective. In: ACDC. 9th IET international conference on AC and DC power transmission, 2010, pp 1–5
17. Van Hertem D, Ghandhari M, Delimar M (2010) Technical limitations towards a Supergrid: a European prospective. In: 2010 IEEE International, Energy Conference and Exhibition (EnergyCon), pp 302–309
18. Van Hertem D, Ghandhari M (2010) Multi-terminal VSC HVDC for the European supergrid: Obstacles. Renew Sustain Energy Rev 14:3156–3163
19. Zhu J, Booth C (2010) Future multi-terminal HVDC transmission systems using voltage source converters. Presented at the 45th international universities power engineering conference (UPEC), 2010 Cardiff, Wales
20. Nakajima T, Irokawa S (1999) A control system for HVDC transmission by voltage sourced converters. In: Power engineering society summer meeting, 1999. IEEE, vol. 2, pp 1113–1119
21. Seki N (2000) Field testing of 53 MVA three-terminal DC link between power system using GTO converters. In: IEEE power engineering society winter meeting 2000, pp 2504–2508
22. Wang J, Li X, Qiu X (2005) Power system research on distributed generation penetration. Autom Electr Power Syst 29:97–99
23. Cole S (2010) Steady-State and Dynamic Modelling of VSC HVDC Systems for Power Systems Simulation, Doctor in de Ingenieurswetenschappen Doctor in de ingenieurswetenschappen, Faculteit Ingenieurswetenschappen, Departement Elektrotechniek. Universiteit Leuven, Belgium
24. Wang W, Barnes M (2014) Power flow algorithms for multi-terminal VSC-HVDC with droop control. IEEE Trans Power Syst 29(4):1721–7930. doi:10.1109/TPWRS.2013.2294198
25. Haileselassie TM, Uhlen K (2010) Primary frequency control of remote grids connected by multi-terminal HVDC. In: General Meeting, 2010 IEEE on power and energy society, pp 1–6
26. Hendriks RL, Paap GC, Kling WL (2007) Control of a multiterminal VSC transmission scheme for connecting offshore wind farms. In: European Wind Energy Conference, Milan, Italy
27. Stagg GW, El-Abiad AH (1968) Computer methods in power system analysis. McGraw-Hill, New York
28. Gonzalez-Longatt F, Roldan J, Burgos-Payán M, Terzija V (2012) Implications of the DC Voltage Control Strategy on the Dynamic Behavior of Multi-terminal HVDC following a Converter Outage, presented at the CIGRE-UK and European T&D network solutions to the challenge of increasing levels of renewable generation. Newcastle-under-Lyme College, Staffordshire, United Kingdom